Environ. Sci. Technol. **2005**, *39,* 4027−4034

Effect of Soil Fulvic Acid on Nickel(II) Sorption and Bonding at the Aqueous-Boehmite (γ-AlOOH) Interface

TIMOTHY J. STRATHMANN* AND SATISH C. B. MYNENI

Department of Geosciences, Princeton University, Guyot Hall, Princeton, New Jersey 08544

The influence of soil-derived fulvic acid (SFA) on Ni^{II} sorption and speciation in aqueous boehmite (γ-AlOOH) suspensions was evaluated using a combination of sorption experiments and Ni K-edge extended X-ray absorption fine structure (EXAFS) spectroscopy measurements. Co-sorption of SFA at the aqueous-boehmite interface modifies both the extent of Ni^{II} sorption as well as the local structure of the sorbing Ni^{II} ions. In SFA-free suspensions, Ni^{II} sorbs by forming inner-sphere bidentate mononuclear complexes with surface aluminol groups. Addition of SFA increases Ni^{II} sorption at pH conditions below the sorption edge observed in SFA-free suspensions and diminishes Ni^{II} sorption at pH above the SFA-free sorption edge. When SFA is co-sorbed to boehmite, Ni^{II} sorbs by forming both ligand-bridging ternary surface complexes (Ni^{II}−SFA−boehmite) as well as surface complexes in which Ni^{II} remains directly bonded to aluminol groups, that is, binary Ni^{II}−boehmite or metal-bridging ternary surface complexes (SFA−Ni^{II}−boehmite). The relative contribution of the individual sorption complexes depends heavily on geochemical conditions; the concentration of ligand-bridging complexes increases with increasing SFA sorption and decreasing pH. The local structure of sorbed Ni^{II} does not change with increasing reaction time even though the extent of sorption continues to increase. This supports a slow uptake mechanism where surface or intraparticle diffusion processes are rate-limiting. This work demonstrates that the association of humic constituents with soil minerals can significantly modify the mechanisms controlling trace metal sorption and transport in heterogeneous aquatic environments.

Introduction

Sorption of Ni^{II} and related transition metals at aqueous-metal oxide interfaces, which are ubiquitous in soil and sedimentary environments (*1*), has been extensively studied using both macroscopic (*2*, *3*) and spectroscopic (*4*, *5*) techniques. The mobility, reactivity, and bioavailability of metal ions are significantly affected by sorption reactions (*6*−*9*). Many mechanisms have been postulated for metal ion sorption, including cation exchange, surface complexation, surface-induced precipitation/coprecipitation, and diffusion into particle micropores (*9*, *10*). Increasingly, in-situ spectroscopic techniques, like extended X-ray absorption fine structure (EXAFS), are being used to differentiate between sorption mechanisms (*10*).

The surfaces of soil minerals are often associated with a range of organic and inorganic substrates, including polymeric humic substances (*11*). Previous work demonstrates that humics contain functional groups that bind strongly with both dissolved metal ions and metal oxide surfaces (e.g., carboxylate, phenolate, amino, thiol) (*12*, *13*). It follows that these constituents can modify metal sorption and speciation in soil solutions. Recently, there has been increased interest in characterizing the mechanisms by which humics and related low molecular weight organic ligands (e.g., citrate, glutamate) affect metal sorption in heterogeneous systems (*14*−*18*).

Conceptually, there are several ways in which humic substances can affect the speciation of trace metals in heterogeneous aquatic environments. First, humics can form aqueous-phase complexes with trace metal ions, thereby competitively diminishing the extent of metal ion sorption and precipitation (*15*, *18*). Alternatively, humics can promote mineral dissolution, potentially modifying the metal-binding properties of the residual surface. Actual sorption of humics to a mineral surface modifies both the long-range electrostatic properties of the aqueous-mineral interface as well as the concentration and molecular characteristics of specific metal-binding sites present. The humic's macromolecular structure also enables simultaneous binding to the sorbing mineral surface and dissolved metal ions (i.e., formation of type B "ligand-bridging" ternary surface complexes) (*15*).

In the present study, batch sorption experiments are combined with Ni K-edge EXAFS spectroscopy measurements to evaluate the effects of soil-derived fulvic acid (SFA) on both the extent of Ni^{II} sorption in aqueous boehmite (γ-AlOOH) suspensions as well as the local structures of the sorbed Ni^{II} ions. EXAFS spectra are interpreted in light of recent work from our lab on the spectral properties of dissolved Ni^{II} complexes with SFA and carboxylate-containing ligands (e.g., acetate, oxalate, citrate) (*19*). While previous work (*18*) reported on the effects of humic acid on Ni^{II} surface precipitation reactions that contribute to sorption at higher Ni^{II} concentrations (*5*, *18*, *20*−*23*), this work reports on the influence of SFA on surface complexation reactions that control Ni^{II} sorption at much lower concentrations that are more representative of uncontaminated soils and sediments. Specific efforts are focused on identifying the effects of key geochemical parameters (pH, concentration of co-sorbed SFA, reaction time) on the mechanisms controlling Ni^{II} sorption.

Experimental Methods

Materials. $NiCl_2 \cdot 6H_2O$, NaCl, NaOH, HCl, HNO_3, MES buffer ($pK_a = 6.1$), MOPS buffer ($pK_a = 7.2$), and HEPES buffer ($pK_a = 7.5$) were purchased from Sigma-Aldrich and Fisher Scientific. Standard grade Elliott soil fulvic acid (2S102F) was obtained from the International Humic Substances Society. Boehmite was selected as a model sorbent because it possesses well-defined properties and has been extensively utilized as a representative aluminum (hydr)oxide phase (*24*, *25*). High-purity synthetic boehmite nanoparticles were obtained from Sasol (Type 14N4-80) and were used without further treatment. The crystal structure was confirmed by powder X-ray diffraction. The five-point N_2 BET specific surface area of boehmite was measured to be 85.6 $m^2\ g^{-1}$.

* Corresponding author present address: Environmental Engineering and Science Program, Dept of Civil and Environmental Engineering, University of Illinois, Newmark Laboratory, MC-250, 205 N. Mathews Ave., Urbana, IL 61801; phone: (217)244-4679; e-mail: strthmnn@uiuc.edu.

10.1021/es0481629 CCC: $30.25
Published on Web 04/23/2005

A pH_{znpc} (point of zero net proton charge) of 8.6 has been previously reported for boehmite (*24*). Prior to use, boehmite was equilibrated in water for at least 1 day to ensure adequate hydration of particle surfaces.

Sorption Experiments. Experiments were conducted to quantify the extent of Ni^{II} and SFA sorption in boehmite suspensions as well as the degree of boehmite dissolution (provided in Supporting Information). Measurements were carried out in both binary (Ni^{II} + boehmite; SFA + boehmite) and ternary (Ni^{II} + SFA + boehmite) batch suspensions that were continually mixed on a rotating shaker table. Solutions and mineral suspensions were prepared using ultrapure deionized water that was boiled and sparged with N_2 to remove dissolved CO_2. However, identical results were obtained using CO_2-equilibrated water. All suspensions were equilibrated under darkness at room temperature.

Kinetic experiments were first conducted to determine an appropriate equilibration time to use in pH-edge experiments. These experiments were carried out at pH 7.0 to both mimic neutral pH environments and to ensure significant undersaturation with respect to $Ni(OH)_2$(s) formation (*26*). Batch reactions of 25 mL were prepared by first mixing stock solutions to achieve the desired concentrations of boehmite (2 g L^{-1} = 171.2 m^2 L^{-1}), SFA (50 mg L^{-1}), pH buffer (0.01 M MOPS), and electrolyte (0.006 M NaCl); the pH buffer + electrolyte provide an ionic strength of 0.01 M. After allowing the suspension to equilibrate for 1 day, 10 or 100 μM Ni^{II} was added to initiate the reactions. Aliquots of the suspension were then periodically collected and filtered (0.2 μM cellulose acetate) to remove boehmite particles and sorbed constituents, and the filtrate was analyzed for dissolved nickel and aluminum. The pH stability was verified by periodic measurement. Tests demonstrated that MOPS buffer did not significantly affect the extent of Ni^{II} sorption; comparable results were obtained for the same conditions (pH 7.0, t_{eq} = 1 day) tested with buffer present (kinetic experiments) and buffer absent (pH-edge experiments).

pH-edge Ni^{II} and SFA sorption experiments were then conducted using equilibration time of 1 day. Twenty-five milliliters of batch reactors were prepared in a similar manner described for kinetic experiments, except that no pH buffers were used; pH was periodically adjusted using HCl and NaOH during the first few hours of equilibration. Suspensions contained 2 g L^{-1} boehmite, 10 or 100 μM Ni^{II}, 0.01 M NaCl, and 10, 50, or 250 mg L^{-1} SFA. After reacting individual suspensions for 1 day, the final pH was measured and then the sample was filtered for analysis of nickel, aluminum, and dissolved organic carbon. Precipitation of $Ni(OH)_2$(s) or other solid phases at pH > 8.0 was prevented by preparing these samples by slowly titrating suspensions initially prepared at lower pH with NaOH and providing sufficient time between titrant additions to allow sorption processes to suppress dissolved Ni^{II} concentrations and maintain a significant degree of undersaturation (*26*).

Dissolved Ni and Al concentrations were determined by inductively coupled plasma-optical emission spectrometry (ICP−OES; Perkin-Elmer Optima 4300 DV), and dissolved organic carbon (DOC) was measured using a Dohrmann Pheonix 8000 Organic Carbon Analyzer. The concentrations of sorbed Ni and SFA were calculated by the difference between the total and measured filtrate concentrations. DOC measurements were not conducted for kinetic experiments because the organic buffer MOPS was used. Replicate samples were run for selected conditions; in all cases the extent of Ni^{II} and SFA sorption varied by ≤5% between replicates, demonstrating good reproducibility of the procedures and analytical methods used.

EXAFS Spectroscopy. Samples for EXAFS analysis were prepared in a similar manner as described for sorption/dissolution experiments. With the exception of suspensions that were reacted for 1 month, all suspensions for EXAFS analysis were prepared at the Stanford Synchrotron Radiation Laboratory during beamtime (SSRL, Menlo Park, CA). This enabled us to obtain spectra as soon as possible after collecting samples and minimizing any storage-related artifacts. Sample pH and ionic strength were maintained using appropriate buffers (MES, MOPS, and HEPES). After reacting suspensions for the desired time period (1 day, 1 week, or 1 month), aqueous- and solid-phases were separated by centrifugation. The supernatant was filtered (0.2 μm) and saved for ICP−OES analysis. EXAFS spectra of the moist solid-phase pastes were then collected after mounting between Kapton tape in 1/16 in. thick Teflon sample holders. ICP−OES analysis of the filtered supernatants demonstrated that the extent of Ni sorption and Al dissolution was consistent with results from earlier batch sorption experiments in which no pH buffers were employed. With the exception of one sample (pH 6, no SFA), the mass of dissolved Ni^{II} present in the pore water of the moist pastes is calculated to be negligible compared to the mass of sorbed Ni^{II}. It follows that the observed spectra reflect the average local structure of the sorbed Ni^{II} species only. The preparation of aqueous Ni^{II}−fulvic acid solutions for EXAFS analysis was described previously (*19*).

Ni K-edge EXAFS spectra were collected on wiggler beamline 4-3 at SSRL and were analyzed using procedures that were described previously in detail (*19*). Spectra were background corrected and converted from energy to *k*-space, and radial structure functions (RSFs) were then obtained by Fourier transforming appropriate regions of the k^3-weighted $\chi(k)$ functions, which varied depending on the quality of the measured spectra. A Kaiser−Bessel window with a smoothing parameter of 5 $Å^{-1}$ was used to suppress artifacts resulting from the finite Fourier filtering ranges used. Ab initio phase and amplitude functions for single and multiple scattering paths were obtained for nickel aluminate spinel ($NiAl_2O_4$) and nickel acetate tetrahydrate standards (*27*−*30*). Structural parameters for Ni^{II} present in each sample were then obtained by fitting spectra in *R*-space using a procedure described previously (*19*). The amplitude reduction factor (S_o^2) was fixed at 0.86 to reduce the number of fitting parameters; this value is considered accurate for metals within 20% (*31*).

Calculations were made to quantify the potential significance of multiple scattering paths to the observed spectra. Simulated RSF features were obtained for FEFF-derived multiple scattering paths of the reference standards. At R < 4.0 Å, the simulated multiple scattering features are small compared to the observed spectra. While this result suggests that multiple scattering processes are not significant in this region of the RSFs, we cannot rule out their contributions. Backscatter features at R > 4 Å are attributed to a combination of multiple scattering processes and single-scattering processes involving distant atomic shells, but no attempt was made to extract structural information from these features.

Results and Discussion

Sorption Kinetics. Figure 1 shows the kinetics of Ni^{II} sorption at pH 7.0 in both pure boehmite suspensions and suspensions preequilibrated with 50 mg L^{-1} SFA. Two-step Ni^{II} sorption behavior is observed. Rapid Ni^{II} uptake during the first day is followed by a much slower sorption process that continues for the next month. The percentage of Ni^{II} sorbed decreases with increasing total Ni^{II} concentration, consistent with a sorption mechanism involving specific metal ion adsorption at a limited number of surface sites (*9*). In the absence of SFA, sorption of 10 μM results in Ni^{II} surface coverages (Γ_{Ni}) ranging from 0 to 0.031 μmol m^{-2}, while sorption of 100 μM Ni^{II} results in surface coverages ranging from 0 to 0.14 μmol m^{-2}. These surface loadings are far below estimates of monolayer coverage (e.g., 1 adsorption site per nm^2 would

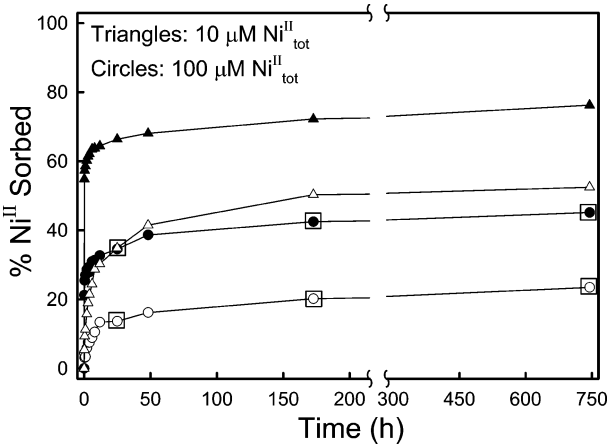

FIGURE 1. Time-dependent sorption of Ni^{II} in aqueous-boehmite suspensions at pH 7.0. Open symbols indicate Ni^{II} sorption in the absence of SFA and closed symbols represent sorption in the presence of 50 mg L^{-1} SFA. Boxes drawn around selected 100 μM Ni^{II}_{tot} samples indicate conditions where EXAFS spectra were obtained (see Tables 1 and 2).

correspond to 1.66 μmol m^{-2}). The extent of Ni^{II} sorption increases significantly when boehmite is preequilibrated with SFA. For example, sorption of 100 μM Ni^{II} more than doubles when 50 mg L^{-1} SFA is present.

pH Sorption Edges. The pH-dependent sorption of Ni^{II} and SFA in boehmite suspensions is shown in Figure 2. In pure boehmite suspensions, Ni^{II} sorption follows typical metal ion adsorption edge behavior (*9*). Negligible sorption occurs at low pH and a sharp increase in sorption from 0 to 100% of the added Ni^{II} concentration occurs between pH 6.5−8.5. The position of the sorption edge (defined by the pH where 50% of Ni^{II} sorbs) for 100 μM Ni^{II} occurs at pH 7.8 (Figure 2A, circles), ~0.7 pH units higher than the edge position observed for 10 μM Ni^{II} (Figure 2B, circles). The maximum surface coverages for the two Ni^{II} concentrations examined are 0.058 and 0.58 μmol m^{-2}, respectively.

Preequilibration of boehmite suspensions with SFA has a marked effect on Ni^{II} sorption. While 10 mg L^{-1} SFA does not noticeably affect the sorption of 10 μM Ni^{II}, 50 mg L^{-1} SFA significantly modifies the sorption trend (Figure 2B). Below pH 7.5, Ni^{II} sorption increases dramatically, while a slight decrease is observed above pH 7.5. Similar effects are observed for 100 μM Ni^{II} but at higher SFA concentrations (Figure 2A). For suspensions preequilibrated with 50 mg L^{-1} SFA, small increases and decreases in the sorption of 100 μM Ni^{II} are observed at pH below and above 8.0, respectively. The effects of 250 mg L^{-1} SFA are much more pronounced, and Ni^{II} sorption exhibits noticeably less pH dependence.

Figure 2C illustrates the effects of pH, SFA concentration, and the presence of Ni^{II} on SFA sorption. Sorption trends characteristic of humic and fulvic acids are observed (*32*, *33*). The percent SFA sorption gradually increases with decreasing pH and decreasing total SFA concentration. Sorption of 50 mg L^{-1} SFA increases from 39 to 75% of the total SFA concentration when pH drops from 8.8 to 4.0. This corresponds to SFA surface coverages (Γ_{SFA}) between 0.11 and 0.22 mg m^{-2}. Sorption of 250 mg L^{-1} SFA ranges from 12 to 39% of the total SFA for the same pH range (Γ_{SFA} from 0.18 to 0.57 mg m^{-2}).

The concentration of carboxylic and phenolic functional groups contained in the structure of sorbed SFA molecules can be estimated by multiplying the sorbed mass concentrations (mg L^{-1} SFA; Figure 2C) times the carbon content of SFA (50.12%) times the carboxylic and phenolic content of SFA reported by Ritchie and Perdue (*34*). Using this procedure, which assumes no SFA fractionation during sorption,

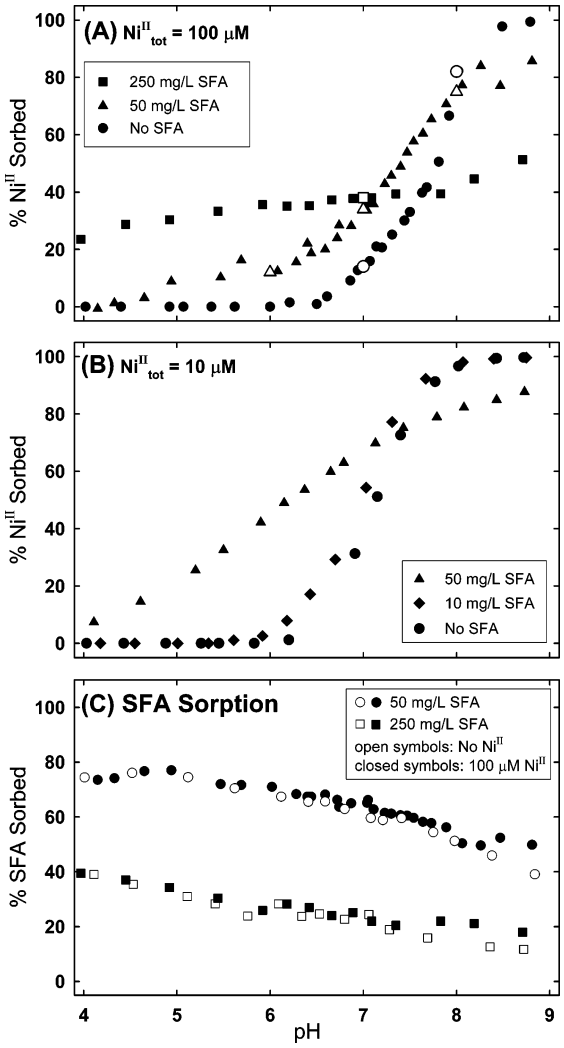

FIGURE 2. pH-dependent sorption of Ni^{II} and SFA in aqueous boehmite suspensions. Panels A and B depict the extent of Ni^{II} sorption in the presence of differing concentrations of SFA. Panel C depicts the extent of SFA sorption in the absence and presence of 100 μM Ni^{II}. Open symbols in panel A represent samples that were also analyzed by EXAFS spectroscopy.

we estimate that the range of sorption measurements for 50 mg L^{-1} SFA correspond to sorbed carboxylic and phenolic concentrations from 130 to 250 μM and from 22 to 43 μM, respectively. For sorption of 250 mg L^{-1} SFA, sorbed carboxylic and phenolic concentration estimates range from 200 to 650 μM and from 34 to 110 μM, respectively. However, because SFA has a macromolecular structure, we presume that only a small fraction of the "sorbed" carboxylic and phenolic groups directly interact with aluminol surface sites, while the remaining "sorbed" groups are free to interact with metal ions and other constituents in the overlying solution.

Unlike the pronounced effects that SFA has on Ni^{II} sorption, the presence of Ni^{II} has little effect on SFA sorption. Below pH 7, sorption of SFA in the absence and presence of 100 μM Ni^{II} is unchanged, and Ni^{II} addition causes only a slight increase in SFA sorption at higher pH. The minimal effect of dissolved metal ions on SFA sorption agrees with previous reports (*33*). Changes in humic sorption imparted by the presence of dissolved metal ions are usually attributed to either the effects that solution-phase metal−humic complexation have on intra- and intermolecular electrostatic interactions of the humics or to formation of metal-bridging (type A) ternary surface complexes (*15*, *35*).

TABLE 1. Boehmite Suspension Conditions Analyzed by EXAFS[a]

sample	t_{eq} (day)	pH_{eq}	$[SFA]_{tot}$ (mg L^{-1})	$[Ni^{II}]_{aq}$ (μM)	$[Ni^{II}]_{sorbed}$ (μM)	Γ_{Ni} (μmol m^{-2})	Γ_{SFA} (mg m^{-2})
			Ni^{II} + Boehmite				
(1)	1	7.0	0	86	14	0.082	0
(2)	7	7.0	0	80	20	0.12	0
(3)	31	7.0	0	76	24	0.14	0
(4)	1	8.0	0	18	82	0.48	0
			Ni^{II} + SFA + Boehmite				
(5)	1	7.0	50	66	34	0.20	0.19
(6)	1	7.0	250	62	38	0.22	0.34
(7)	1	8.0	50	25	75	0.44	0.15
(8)	1	6.0	50	88	12	0.070	0.21
(9)	7	7.0	50	57	43	0.25	na[b]
(10)	31	7.0	50	55	45	0.26	na[b]

[a] All samples contain $[Ni^{II}]_{tot}$ = 100 μM and ionic strength = 0.01 M. [b] Extent of SFA sorption not measured in long-term kinetic samples because the organic pH buffers interfere with TOC measurements.

EXAFS Measurements. EXAFS spectra were measured for both aqueous solutions containing Ni^{II} and SFA and for solid-phase samples collected from boehmite suspensions that correspond to conditions indicated in Figure 1 (boxed symbols) and Figure 2A (open symbols). A detailed list of the suspension conditions examined is provided in Table 1. Although high-resolution XANES (X-ray absorption near-edge structure) spectra were not collected for boehmite paste samples, the energy and features of the main absorption edge are consistent with octahedrally coordinated Ni ions in the +2 oxidation state, as was discussed in a previous publication (*19*).

Aqueous Ni^{II}−SFA Complexes. EXAFS spectra for aqueous solutions containing Ni^{II} and SFA were discussed in detail in a previous publication (*19*). Briefly, spectral fits are consistent with Ni^{II} ions possessing an octahedral inner coordination shell of six oxygen (or possibly nitrogen) atoms located at ∼2.04 Å and one or more carbon atoms located at 2.8−2.9 Å (See Table 2). These parameters agree with earlier reports of Ni^{II}−humic complexes (*18*, *36*) and are similar to those obtained for inner-sphere Ni^{II} complexes with simple monocarboxylate (e.g., acetate) and weakly chelating polycarboxylate (e.g., succinate) and mixed carboxylate/phenolate (e.g., salicylate) ligands, suggesting that Ni^{II} forms similar complexes with these functional groups contained in the SFA structure.

Ni^{II} Sorption on Boehmite. Before the effects of SFA can be considered, it is appropriate to evaluate the spectra of sorbed Ni^{II} in pure boehmite suspensions. EXAFS spectra were collected at different equilibration times (1 day, 1 week, and 1 month) and different pH conditions (pH 7, 8) (Table 1). k^3-weighted χ functions and the corresponding RSFs, uncorrected for phase shift (∼+0.4 Å), are shown in Figure 3. Both the χ functions and the RSFs differ from dissolved $Ni(H_2O)_6^{2+}$, suggesting that sorption to boehmite markedly affects the local structure of Ni^{II}. The smoothly decreasing oscillatory pattern in the χ function for $Ni(H_2O)_6^{2+}$ is replaced by distinct asymmetry in the pattern for sorbed Ni^{II}, which is also offset slightly from $Ni(H_2O)_6^{2+}$ (see vertical dashed line). Splitting in the first oscillation near 4 $Å^{-1}$ (see arrow) is also observed for sorbed Ni^{II} but is absent for $Ni(H_2O)_6^{2+}$. Yamaguchi and co-workers attributed similar features to multiple scattering processes involving Al atoms within the structure of the sorbing mineral, gibbsite (*37*). Correspondingly, the RSF for sorbed Ni^{II} shows clear evidence for changes in the local coordination environment. Although all samples contain a similar first-shell peak at ∼1.63 Å (uncorrected for phase shift), sorbed Ni^{II} samples contain an additional peak between 2 and 3.5 Å. This demonstrates the presence of significant backscatterers beyond the first atomic shell. The spectral features are largely invariant with changes in equilibration time and pH, indicating that the local structure of sorbed Ni^{II} ions does not change even as the extent of sorption changes (see Figures 1 and 2). Attempts were made to fit the second-shell RSF features using Ni−Al and Ni−Ni single-scattering paths, but only the former proved successful. Structural parameters obtained from two-shell fits indicate the presence of six oxygen atoms at 2.06 Å and one or more aluminum atoms at 2.97−2.98 Å. Inclusion of an additional

TABLE 2. EXAFS Spectra Fitting Results[a]

	Aqueous Samples first shell (Ni−O)[b]			second shell[c]				
composition	CN	R (Å)	σ^2 ($Å^2$)	CN	R (Å)	σ^2 ($Å^2$)	ΔE_o (eV)[d]	% res[e]
50 mM $Ni(H_2O)_6^{2+}{}_{aq}$ (pH 2, NO_3^- salt)	6.0	2.05	0.005				3.10	5.7
1 mM Ni^{II} + 2 g L^{-1} SFA, pH 7.0	5.5	2.04	0.006	3.1 C	2.85	0.009	2.58	2.8
1 mM Ni^{II} + 4 g L^{-1} SFA, pH 7.0	6.6	2.03	0.007	2.1 C	2.87	0.006	2.96	4.2
1 mM Ni^{II} + 2 g L^{-1} SFA, pH 5.5	5.4	2.04	0.005	3.5 C	2.80	0.011	2.62	5.3
1 mM Ni^{II} + 2 g L^{-1} SFA, pH 8.5	5.6	2.04	0.006	1.8 C	2.84	0.007	2.08	5.1

				Boehmite Suspensions first shell (Ni−O)[b]			second shell[c]				
no.	t_{eq} (days)	pH	$[SFA]_{tot}$ (mg L^{-1})	CN	R (Å)	σ^2 ($Å^2$)	CN	R (Å)	σ^2 ($Å^2$)	ΔE_o (eV)[d]	% res[e]
(1)	1	7.0	0	6.0	2.06	0.005	1.9 Al	2.98	0.004	4.51	9.0
(2)	7	7.0	0	6.1	2.06	0.006	1.8 Al	2.98	0.003	4.25	8.4
(3)	31	7.0	0	5.8	2.06	0.005	2.2 Al	2.97	0.004	4.70	9.4
(4)	1	8.0	0	6.0	2.06	0.006	1.9 Al	2.97	0.004	4.36	8.8
(5)	1	7.0	50	6.2	2.05	0.006				3.92	10.7
(6)	1	7.0	250	6.0	2.05	0.006				3.82	8.4
(7)	1	8.0	50	5.9	2.06	0.006	1.0 Al	2.98	0.003	3.81	7.0
(8)	1	6.0	50	6.1	2.04	0.006				3.08	14.1
(9)	7	7.0	50	6.1	2.05	0.006				4.17	8.3
(10)	31	7.0	50	5.8	2.05	0.006				3.64	14.8

[a] Single and multishell fits carried out in R-space. [b] Error estimates for first-shell fitted parameters: CN ± 20%, R ± 0.02 Å, σ^2 ± 20−30%. [c] Error estimates for second-shell fitted parameters: CN ± 40%, R ± 0.05 Å, σ^2 ± 20−30%. [d] ΔE_o values relative to 8345 eV. [e] Percent residual between measured and fit spectra calculated from 0.95−3.0 Å in R space.

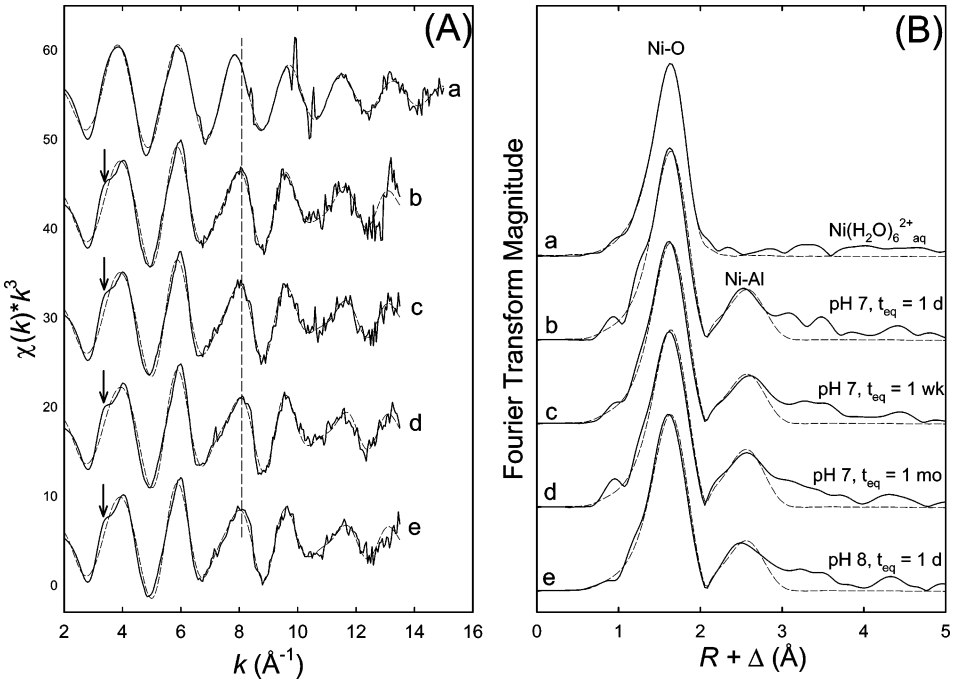

FIGURE 3. EXAFS data of Ni^{II} sorbed at the aqueous-boehmite interface in the absence of SFA. The spectrum of dissolved $Ni(H_2O)_6^{2+}$ is shown for comparison (trace a). (A) Background-subtracted k^3-weighted $\chi(k)$ functions (EXAFS). (B) Radial structure functions, uncorrected for phase shift. Solid and dashed lines represent experimental spectra and *R*-space fits, respectively. Spectra are of wet pastes collected from aqueous suspensions by centrifugation. Detailed sample conditions are provided in Table 1 and structural parameters obtained from spectral fits are provided in Table 2.

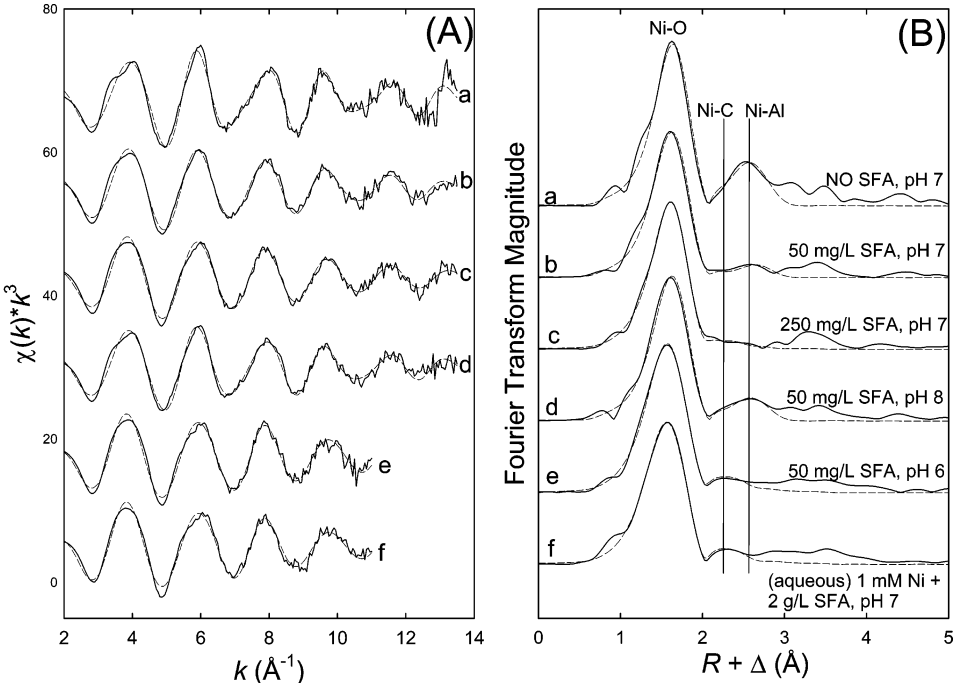

FIGURE 4. Effect of SFA on the EXAFS measurements of Ni^{II} sorbed at the aqueous-boehmite interface. The spectra of an aqueous Ni^{II}−SFA solution is shown for comparison (trace f). (A) Background-subtracted k^3-weighted $\chi(k)$ functions (EXAFS). (B) Radial structure functions, uncorrected for phase shift. Spectra shown are for samples that were reacted for 1 d. Solid and dashed lines represent experimental spectra and *R*-space fits, respectively. Detailed sample conditions are provided in Table 1 and structural parameters obtained from spectral fits are provided in Table 2.

Ni−Al, Ni−Ni, or Ni−O single scattering path did not result in improved fits of the second-shell region of the RSF or fits of the residual RSF spectra obtained from two-shell fits.

Ni^{II} Sorption in the Presence of SFA. EXAFS spectra were also collected of suspensions equilibrated with SFA prior to adding Ni^{II} (Table 1). Figure 4 shows representative χ functions and the corresponding RSFs, which provide evidence for a change in the local coordination environment when SFA is added. The asymmetric features in the χ functions observed in pure boehmite suspensions are greatly reduced, and spectra appear more similar to aqueous Ni^{II}−SFA solutions (*19*). While the first peak in the RSFs is similar for all samples, spectral intensity between 2 and 3 Å is greatly reduced for sorbed Ni^{II} samples when SFA is present, despite

the fact that the SFA increases the extent of Ni^{II} sorption for pH 6−7 (see Figure 2A). This loss in backscatter intensity indicates that second-shell Al^{III} atoms are being replaced by weaker backscattering atoms such as carbon from the SFA structure. With the exception of a single sample at pH 8, second-shell spectral fits using a single Ni−C or Ni−Al single scattering path, or a combination of the two paths, proved unsuccessful. This is consistent with an earlier report in which the difficulty of fitting weak Ni−C backscatter features was discussed at length (*19*). The pH 8 sample (trace d in Figure 4) was successfully fit using a Ni−Al single scattering path, but the fit-derived value of CN_{Ni-Al} is 50% lower than the values obtained for Ni^{II} sorbed in pure boehmite suspensions (samples 1−4). This finding suggests that multiple species contribute to Ni^{II} sorption at pH 8, some with spectral features similar to those measured in SFA-free suspensions and some with spectral features similar to those observed in aqueous Ni^{II}−SFA solutions.

Sorption Mechanism. Complementary results from sorption experiments and spectroscopy measurements support Ni^{II} sorption via formation of binary and ternary Ni^{II} surface complexes at the aqueous-boehmite interface.

Ni^{II} Sorption in Pure Boehmite Suspensions. In the absence of SFA, experimental results are consistent with Ni^{II} sorption via formation of inner-sphere surface complexes with aluminol groups on the boehmite surface. The extent of Ni^{II} sorption increases from 0 to 100 percent over a narrow pH window, and the position of the adsorption edge varies with total Ni^{II} concentration in the suspension (Figure 2). EXAFS spectral fits indicate the presence of one or more aluminum atoms in the second atomic shell surrounding sorbed Ni^{II} ions. Fit-derived Ni−Al bond distances are considered more accurate than the second-shell coordination number estimates and therefore are better indicators of the structures of surface complexes. The fit-derived Ni−O and Ni−Al bond distances reported in Table 2 (∼2.06 Å and ∼2.98 Å, respectively) are most consistent with a bidentate mononuclear surface complex (depicted below). This mode of bonding involves edge-sharing between the first-shell octahedra of the sorbing Ni^{II} ion and the Al^{III} ion

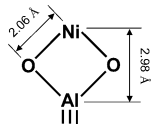

contained in the boehmite surface. Monodentate mononuclear and bidentate binuclear bonding structures are indirectly ruled out because these structures require larger Ni−Al bonding distances (estimates of >3.2 Å and >3.4 Å, respectively).

Measured spectral features also rule out Ni^{II} precipitation as a significant sorption mechanism under conditions examined here. Sparks and co-workers report that surface precipitation of Ni^{II} hydroxide and mixed Ni−Al layered double hydroxide (LDH) phases is a dominant sorption mechanism in several Al^{III}− and Si^{IV}−mineral suspensions (e.g., phyllosilicates, low surface area gibbsite, amorphous silica) (*5*, *18*, *20*−*23*). However, characteristic spectral features of the surface precipitates, most notably a beat pattern in χ functions between 8 and 9 $Å^{-1}$ and second-shell RSF peaks centered near ∼2.8 Å, are absent in spectra reported here. Instead, spectra for Ni^{II} sorbed to boehmite are similar to those reported by Yamaguchi et al. (*37*) for Ni^{II} sorbed to a high surface area gibbsite phase (96 $m^2\ g^{-1}$) at reaction times of 1 day or shorter and attributed by these authors to formation of surface complexes. Furthermore, spectra for Ni^{II} sorbed on boehmite are invariant with reaction time, even though the extent of Ni^{II} sorption continues to increase for more than a month (Figure 1). This finding is contradictory with reports of surface-induced $Ni(OH)_2$(s) and Ni−Al LDH precipitation, where continued uptake of Ni^{II} is accompanied by growth of second-shell Ni−Ni backscatter features (*23*). Instead, the time-invariant nature of spectra is similar to earlier reports in which slow metal uptake was attributed to mechanisms involving adsorption of mononuclear metal species where slow surface or intraparticle diffusion processes are rate-limiting (*38*, *39*). It is also worth pointing out, though, that the total Ni^{II} concentrations used in this study (0.1 mM) are 15 to 30-fold lower than those typically used by Sparks and co-workers (1.5−3 mM) (*5*, *20*−*23*, *37*), an important factor that may contribute to differences in the dominant sorption mechanisms is observed. Further research is needed to establish exactly how the concentration of Ni^{II} affects the mechanism of sorption to important soil mineral phases.

Effect of SFA on Ni^{II} Sorption. In the presence of SFA, Ni^{II} sorbs by forming a mixture of surface complexes, some containing Ni^{II}−aluminol bonds (e.g., binary Ni^{II}−boehmite and type A metal-bridging ternary surface complexes) and some lacking direct Ni^{II}−aluminol bonding (e.g., type B ligand-bridging ternary surface complexes), and the relative contribution of the individual complexes varies with solution composition. Sorption trends agree with earlier reports of metal sorption in metal oxide suspensions containing humic substances (*33*, *40*, *41*). Addition of SFA increases Ni^{II} sorption at lower pH and decreases sorption at higher pH. Enhanced metal sorption at low pH, where humic sorption is greatest, has been attributed to formation of type B ternary surface complexes where the metal ion is complexed by humic molecules that are simultaneously adsorbed to the mineral surface (*40*, *41*). Alternatively, humic-promoted metal sorption is sometimes attributed to a reduction in the net positive surface charge caused by adsorption of negatively charged humic molecules, which leads to more favorable electrostatic interactions with dissolved metal ions (i.e., lowers the pH_{znpc} of the mineral) (*42*). Reductions in metal sorption at high pH are generally attributed to formation of dissolved metal−humic complexes that compete with sorption processes (*33*, *40*, *41*).

At pH 6 and 7, EXAFS spectra are consistent with the predominance of ligand-bridging Ni^{II}−SFA−boehmite ternary complexes. The intensity of second-shell spectral features decrease markedly in comparison to SFA-free boehmite samples, appearing similar to aqueous Ni^{II}−SFA complexes (Figure 4) and suggesting that Ni^{II} may be complexed by sorbed SFA molecules instead of directly to the boehmite surface. At pH 8, a successful fit of spectra using a Ni−Al backscatter path indicates that formation of sorbed Ni^{II} species possessing Ni^{II}−aluminol bonds is also important at higher pH. Because Ni−C backscattering is weak in Ni^{II}−SFA complexes (*19*), we are unable to differentiate between simple binary Ni^{II}−boehmite surface complexes and type A Ni^{II}−bridging ternary surface complexes. The varying contribution of binary and ternary surface complexes to overall Ni^{II} sorption at different pH agrees with expected surface complexation trends. That is, type B ternary surface complexes predominate at lower pH and higher SFA concentrations, while binary Ni^{II}−boehmite surface complexes or type A ternary surface complexes predominate at higher pH and lower SFA concentrations (*15*).

Complementary macroscopic and spectroscopic experiments reported here and in a prior study (*19*) demonstrate that Ni^{II} forms inner-sphere complexes with boehmite surfaces as well as natural organic constituents and that both binary and ternary interactions between these constituents need to be considered to accurately predict Ni^{II} speciation in complex heterogeneous aquatic environments. Results reported here do not address the nature of the SFA−boehmite sorption interaction, but previous studies report that humic

substances and ligands possessing similar Lewis base donor groups sorb to aqueous-aluminum oxide interfaces by a combination of outer-sphere interactions (hydrogen bonding, long-range electrostatic) and inner-sphere complexation reactions (*24*, *43*, *44*).

Acknowledgments

This work was supported by NSF and DOE. We thank SSRL staff for their assistance with EXAFS measurements. Valuable comments and discussion were provided by F. M. M. Morel (Princeton) and three anonymous reviewers. W. J. Weiss and R. Spinette (Johns Hopkins) assisted with DOC measurements.

Supporting Information Available

Boehmite dissolution data measured during Ni^{II} and SFA sorption experiments. This material is available free of charge via the Internet at http://pubs.acs.org.

Literature Cited

(1) McBride, M. B. *Environmental Chemistry of Soils*; Oxford University Press: New York, 1994.
(2) Coughlin, B. A.; Stone, A. T. Nonreversible adsorption of divalent metal ions (Mn^{II}, Co^{II}, Ni^{II}, Cu^{II}, and Pb^{II}) onto goethite: effects of acidification, Fe^{II} addition, and picolinic acid addition. *Environ. Sci. Technol.* **1995**, *29*, 2445−2455.
(3) Trivedi, P.; Axe, L. Predicting divalent metal sorption to hydrous Al, Fe, and Mn oxides. *Environ. Sci. Technol.* **2001**, *35*, 1779−1784.
(4) Roe, A. L.; Hayes, K. F.; Chisholm-Brause, C.; Brown, G. E.; Parks, G. A.; Hodgson, K. O.; Leckie, J. O. In situ X-ray absorption study of lead ion surface complexes at the goethite−water interface. *Langmuir* **1991**, *7*, 367−373.
(5) Scheidegger, A. M.; Lamble, G. L.; Sparks, D. L. Investigation of Ni sorption on pyrophyllite: an XAFS study. *Environ. Sci. Technol.* **1996**, *30*, 548−554.
(6) Hudson, R. J. M. Which aqueous species control the rates of trace metal uptake by aquatic biota? Observations and predictions of non-equilibrium effects. *Sci. Total Environ.* **1998**, *219*, 95−115.
(7) Buerge, I. J.; Hug, S. J. Influence of mineral surfaces on chromium(VI) reduction by iron(II). *Environ. Sci. Technol.* **1999**, *33*, 4285−4291.
(8) Xue, H. B.; Sigg, L.; Gächter, R. Transport of Cu, Zn, and Cd in a small agricultural catchment. *Water Res.* **2000**, *34*, 2558−2568.
(9) Stumm, W. *Chemistry of the Solid−Water Interface: Processes at the Mineral-Water and Particle−Water Interface in Natural Systems*; John Wiley and Sons: New York, 1992.
(10) Sparks, D. L.; Scheidegger, A. M.; Strawn, D. G.; Scheckel, K. G. Kinetics and mechanisms of metal sorption at the mineral−water interface. In *Mineral−Water Interfacial Reactions: Kinetics and Mechanisms*; Sparks, D. L., Grundl, T. J., Eds.; American Chemical Society: Washington, DC, 1998; pp 108−135.
(11) Thurman, E. M. *Organic Geochemistry of Natural Waters*; Martinus Nijhoff Publishers: Dordrecht, The Netherlands, 1985.
(12) Davies, G.; Fataftah, A.; Cherkasskiy, A.; Ghabbour, E. A.; Radwan, A.; Jansen, S. A.; Kolla, S.; Paciolla, M. D.; Sein, L. T.; Buermann, W.; Balasubramanian, M.; Budnick, J.; Xing, B. Tight metal binding by humic acids and its role in biomineralization. *J. Chem. Soc., Dalton Trans.* **1997**, 4047−4060.
(13) Davis, J. A. Adsorption of natural dissolved organic matter at the oxide/water interface. *Geochim. Cosmochim. Acta* **1982**, *46*, 2381−2393.
(14) Schindler, P. Co-adsorption of metal ions and organic ligands: formation of ternary surface complexes. In *Mineral−Water Interface Geochemistry*; Hochella, M. F., White, A. F., Eds.; Mineralogical Society of America: Washington, DC, 1990; Vol. 23, pp 281−307.
(15) Fein, J. B. The effects of ternary surface complexes on the adsorption of metal cations and organic acids onto mineral surfaces. In *Water−Rock Interactions, Ore Deposits, and Environmental Geochemistry*; Hellmann, R., Wood, S. A., Eds.; Geochemical Society: St. Louis, MO, 2002.
(16) Fitts, J. P.; Persson, P.; Brown, G. E.; Parks, G. A. Structure and bonding of Cu(II)−glutamate complexes at the γ-Al_2O_3−water interface. *J. Colloid Interface Sci.* **1999**, *220*, 133−147.
(17) Alcacio, T. E.; Hesterberg, D.; Chou, J. W.; Martin, J. D.; Beauchemin, S.; Sayers, D. E. Molecular scale characteristics of Cu(II) bonding in goethite−humate complexes. *Geochim. Cosmochim. Acta* **2001**, *65*, 1355−1366.
(18) Nachtegaal, M.; Sparks, D. L. Nickel sequestration in a kaolinite-humic acid complex. *Environ. Sci. Technol.* **2003**, *37*, 529−534.
(19) Strathmann, T. J.; Myneni, S. C. B. Speciation and complexation in aqueous nickel(II)−carboxylate and Ni(II)−humic solutions: combined ATR-FTIR and XAFS analysis. *Geochim. Cosmochim. Acta* **2004**, *68*, 3441−3458.
(20) Scheinost, A. C.; Ford, R. G.; Sparks, D. L. The role of Al in the formation of secondary Ni precipitates on pyrophyllite, gibbsite, talc, and amorphous silica: a DRS study. *Geochim. Cosmochim. Acta* **1999**, *63*, 3193−3203.
(21) Scheinost, A. C.; Sparks, D. L. Formation of layered single- and double-metal hydroxide precipitates at the mineral/water interface: a multiple-scattering XAFS analysis. *J. Colloid Interface Sci.* **2000**, *223*, 167−178.
(22) Scheidegger, A. M.; Fendorf, M.; Sparks, D. L. Mechanisms of nickel sorption on pyrophyllite: macroscopic and microscopic approaches. *Soil Sci. Soc. Am. J.* **1996**, *60*, 1763−1772.
(23) Scheidegger, A. M.; Strawn, D. G.; Lamble, G. L.; Sparks, D. L. The kinetics of mixed Ni−Al hydroxide formation on clay and aluminum oxide minerals: a time-resolved XAFS study. *Geochim. Cosmochim. Acta* **1998**, *62*, 2233−2245.
(24) Nordin, J.; Persson, P.; Laiti, E.; Sjöberg, S. Adsorption of *o*-phthalate at the water−boehmite (γ-AlOOH) interface: evidence for two coordination modes. *Langmuir* **1997**, *13*, 4085−4093.
(25) Axe, K.; Persson, P. Time-dependent surface speciation of oxalate at the water−boehmite (γ-AlOOH) interface: implications for dissolution. *Geochim. Cosmochim. Acta* **2001**, *65*, 4481−4492.
(26) Martell, A. E.; Smith, R. M.; Motekaitus, R. J. *Critically Selected Stability Constants of Metal Complexes Database*, Version 4.0; U.S. Department of Commerce, National Institute of Standards and Technology: Gaithersbug, MD, 1997.
(27) Nicolai, B.; Kearley, G. J.; Johnson, M. R.; Fillaux, F.; Suard, E. Crystal structure and low-temperature methyl-group dynamics of cobalt and nickel acetates. *J. Chem. Phys.* **1998**, *109*, 9062−9074.
(28) Ravel, B. ATOMS: crystallography for the X-ray absorption spectroscopist. *J. Synchrotron Radiat.* **2001**, *8*, 314−316.
(29) Ankudinov, A. L.; Ravel, B.; Rehr, J. J.; Conradson, S. D. Real space multiple scattering calculation and interpretation of X-ray absorption near edge structure. *Phys. Rev. B* **1998**, *58*, 7565.
(30) Roelofsen, J. N.; Peterson, R. C.; Raudsepp, M. Structural variation in nickel aluminate spinel ($NiAl_2O_4$). *Am. Mineral.* **1992**, *77*, 522−528.
(31) Rehr, J. J.; Mustre de Leon, J.; Zabinsky, S. I.; Albers, R. C. Theoretical X-ray absorption fine structure standards. *J. Am. Chem. Soc.* **1991**, *113*, 5135−5140.
(32) Filius, J. D.; Lumsdon, D. G.; Meeussen, J. C. L.; Hiemstra, T.; Van Riemsdijk, W. H. Adsorption of fulvic acid on goethite. *Geochim. Cosmochim. Acta* **2000**, *64*, 51−60.
(33) Christl, I.; Kretzschmar, R. Interaction of copper and fulvic acid at the hematite−water interface. *Geochim. Cosmochim. Acta* **2001**, *65*, 3435−3442.
(34) Ritchie, J. D.; Perdue, E. M. Proton-binding study of standard and reference fulvic acids, humic acids, and natural organic matter. *Geochim. Cosmochim. Acta* **2003**, *67*, 85−96.
(35) Ali, M. A.; Dzombak, D. A. Effects of simple organic acids on sorption of Cu^{2+} and Ca^{2+} on goethite. *Geochim. Cosmochim. Acta* **1996**, *60*, 291−304.
(36) Xia, K.; Bleam, W.; Helmke, P. A. Studies of the nature of binding sites of first row transition elements bound to aquatic and soil humic substances using X-ray absorption spectroscopy. *Geochim. Cosmochim. Acta* **1997**, *61*, 2223−2235.
(37) Yamaguchi, N. U.; Scheinost, A. C.; Sparks, D. L. Influence of gibbsite surface area and citrate on Ni sorption mechanisms at pH 7.5. *Clays Clay Miner.* **2002**, *50*, 784−790.
(38) Scheinost, A. C.; Abend, S.; Pandya, K. I.; Sparks, D. L. Kinetic controls on Cu and Pb sorption by ferrihydrite. *Environ. Sci. Technol.* **2001**, *35*, 1090−1096.
(39) Trivedi, P.; Axe, L.; Tyson, T. A. XAS studies of Ni and Zn sorbed to hydrous manganese oxide. *Environ. Sci. Technol.* **2001**, *35*, 4515−4521.
(40) Tipping, E.; Griffith, J. R.; Hilton, J. The effect of adsorbed humic substances on the uptake of copper(II) by goethite. *Croat. Chem. Acta* **1983**, *56*, 613−621.
(41) Davis, J. A. Complexation of trace metals by adsorbed natural organic matter. *Geochim. Cosmochim. Acta* **1984**, *48*, 679−691.

(42) Tipping, E.; Cooke, D. The effects of adsorbed humic substances on the surface charge of goethite (α-FeOOH) in freshwaters. *Geochim. Cosmochim. Acta* **1982**, *46*, 75−80.
(43) Yoon, T. H.; Johnson, S. B.; Brown, G. E. Adsorption of Suwannee River fulvic acid on aluminum oxyhydroxide surfaces: an in situ ATR-FTIR study. *Langmuir* **2004**, *20*, 5655−5658.
(44) Johnson, S. B.; Yoon, T. H.; Kocar, B. D.; Brown, G. E. Adsorption of organic matter at mineral/water interfaces. 2. Outer-sphere adsorption of maleate and implications for dissolution processes. *Langmuir* **2004**, *20*, 4996−5006.

Received for review November 22, 2004. Revised manuscript received March 25, 2005. Accepted March 25, 2005.

ES0481629